Recent Advances in Enhancing Shell-Side Condensation in Refrigerant Condensers

Honda, Hiroshi
Institute of Advanced Material Study, Kyushu University

https://doi.org/10.15017/6653

出版情報：九州大学機能物質科学研究所報告. 8 (1), pp.149-162, 1994-11-10. Institute of Advanced Material Study , Kyushu University
バージョン：
権利関係：

Rep. Inst. Adv. Mat.
Study, Vol. 8, No. 1
pp. 149~162(1994)

Recent Advances in Enhancing Shell-Side Condensation in Refrigerant Condensers

Hiroshi HONDA

This paper reviews recent advances that have been made in enhancing film condensation of fluorocarbon refrigerants in a bundle of horizontal tubes. The emphasis in the discussion is on the effects of fin geometry, vapor shear and condensate inundation. It is shown that the fin geometry is an important factor that controls the heat transfer performance. The effect of vapor shear is much smaller for a finned tube than for a smooth tube. The effect of condensate inundation is more marked for a three-dimensional fin tube than for a two-dimensional fin tube. Also, the effect is more marked for an in-line tube bundle than for a staggered tube bundle. For a two-dimensional fin tube with and without the effect of vapor shear and for a bundle of two-dimensional fin tubes with negligible vapor shear, several theoretical models exist that can predict the heat transfer coefficient with sufficient accuracy. The theoretical model can be used to optimize the fin geometry.

1. Introduction

Shell-side condensers are used in the refrigeration, air-conditioning and heat pump equipments of medium to large capacity. Since halocarbon refrigerants used in these systems have a low liquid thermal conductivity, finned tubes are commonly used to enhance shell-side condensation. Thus, the development of a high performance shell-side condenser depends largely on the optimization of fin geometry.

Table 1 is a listing of factors that affect the heat transfer coefficient during condensation of pure vapors in the shell-side condenser. The phenomenon is complicated by the combined effects of these factors. Numerous experimental and theoretical studies that dealt with the effects of these factors have been reported. Webb[1] provides a state of the art survey of shell-side condensation in refrigerant condensers. Webb[2], Marto[3] and Sukhatme[4] give literature reviews that are focused on the enhancement of condensation by use of finned tubes. While these reviews provide a large amount of information on the effects of various factors on the condensation of refrigerants in a bundle of smooth tubes and on a single finned tube, information is rather limited for a bundle of finned tubes. Also, it should be mentioned that only a small number of experimental data are currently available in the open literature

Received June 24, 1994
Dedicated to Professor Tetsu Fujii on the occasion of his retirement

Table 1 Factors that affect condensation heat transfer of pure refrigerants in a shell-side condenser.

Item	Factor
Tube	Geometry: Smooth tube; Finned tube (Fin shape; Fin dimensions)
	Arrangement: In-line bundle; Staggered bundle
	Number of vertical rows
	Diameter
	Pitch-to-diameter ratio
	Material
Vapor	Velocity
	Flow direction
	Vapor-to-surface temperature difference
	Degree of superheat
	Substance
Condensate	Inundation rate
	Mode of inundation
Coolant	Number of passes
	Pass-circuiting

regarding the heat transfer performance of alternative refrigerants.

The objective of this paper is to review recent advances that have been made in enhancing shell-side condensation in refrigerant condensers. The emphasis in the discussion is on the effects of fin geometry, vapor shear and condensate inundation.

2. Theoretical Results

2. 1. Effect of fin geometry

Commercially available finned tubes are divided into two categories; i.e. a two-dimensional fin tube and a three-dimensional fin tube. The three-dimensional fin tube can utilize the surface tension effect (i.e. local thinning of condensate film at the corner of fin surface) more efficiently than the two-dimensional fin tube. However, recent experimental results show that the decrease in the heat transfer coefficient due to condensate inundation is more marked for the three-dimensional fin tube (see section 3. 2). Therefore, the two-dimensional fin tube with an optimum fin geometry is best suited for a large shell-side condenser.

Figure. 1 shows a physical model and coordinates used for the analysis of film condensation on a horizontal two-dimensional fin tube. In Fig. 1, h denotes the fin height, t the fin thickness, p the fin pitch and d_0 the tube diameter to the fin tip. The condensate generated on the fin surface is driven by combined surface tension and gravity forces toward the fin root and then flows down the groove between adjacent fins by gravity. The cross-sectional area of a thick condensate film in the groove is determined by a balance of condensates

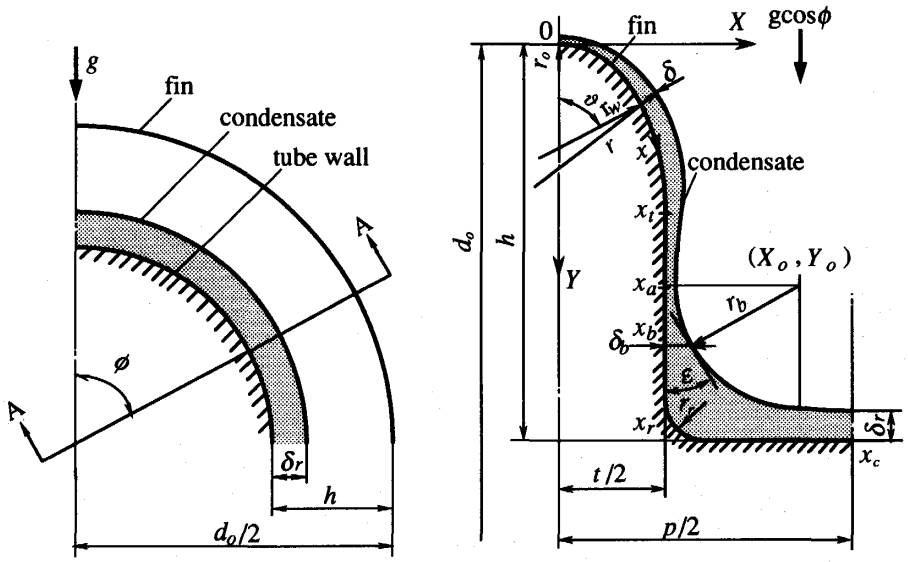

(a) Tube cross section (b) A-A cross section

Fig. 1 Physical model and coordinates.

flowing into the groove and flowing circumferentially down the groove.

Assuming the Nusselt[5] type condensation and $h \ll d_0$, the basic equation for a thin condensate film is written as

$$\frac{2\rho_l g}{3\nu_l d_0}\frac{\partial}{\partial\phi}\left(\delta^3\sin\phi\right)+\frac{1}{3\nu_l}\frac{\partial}{\partial x}\left\{\left[\rho_l g_x-\sigma\frac{\partial}{\partial x}\left(\frac{1}{r}\right)\right]\delta^3\right\}=\frac{\lambda_l(T_s-T_w)}{\delta h_{fg}} \tag{1}$$

where δ is the condensate film thickness, ϕ is the angle measured from the tube top, x is the curvilinear coordinate measured along the surface from the fin tip, $r=(\delta,\partial\delta/\partial x,\partial^2\delta/\partial x^2)$ is the radius of curvature of the condensate surface, g is the gravitational acceleration, g_x is the x -component of gravity, T_s is the saturation temperature, T_w is the local fin temperature, σ is the surface tension, h_{fg} is the latent heat of evaporation, and ν_l, $\rho_l\lambda_l$ are the kinematic viscosity, density and thermal conductivity of condensate, respectively.

The boundary conditions for the thin film on the fin surface are

$$\partial\delta/\partial\phi=0 \text{ at } \phi=0 \tag{2}$$

$$\partial\delta/\partial x=0 \text{ and } \partial(1/r)/\partial x=0 \text{ at } x=0 \tag{3}$$

$$\partial\delta/\partial x=\tan\varepsilon \text{ and } r=-r_b \text{ at } x=x_b \tag{4}$$

where x_b is the connecting point between the thin film and the thick film. Similar boundary conditions hold for the thin condensate film on the fin root tube surface. It is relevant to note here that the basic equation for a vertical finned tube is obtained by putting $\sin\phi=1$, $g_x=1$ and $d_0\partial\phi/2\rightarrow\partial y$ in equation (1), where y denotes the coordinate measured vertically downward from the tube top. Relative importance of the gravity and surface tension forces acting on the thin condensate film depends on the fin dimensions. Generally, the surface tension effect becomes more important as the fin dimensions decrease.

Conventional two-dimensional fin tubes (i.e. low-fin tubes) have a nearly trapezoidal fin cross-section. For this class of finned tube, Beatty and Katz[6] proposed the first theoretical model of film condensation that assumed gravity drained condensate flow. Recently, several theoretical models that took account of both the gravity and surface tension effects with different degree of completeness have been proposed.[7~10]

Gregorig[11] noticed the importance of surface tension in enhancing film condensation on a vertical finned surface. Since then, several advanced fin shapes that can utilize the surface tension effect efficiently have been proposed. Table 2 is a summary of fin/interface shapes taken up for theoretical consideration. In Table 2, r_w denotes the radius of curvature of the fin surface, r_0 the fin tip radius, θ the angle measured from the fin tip, and subscript t denotes the end of the convex arc (see Fig. 1). Most of the fin shapes listed in Table 2 (excepting the triangular and rectangular fins) are characterized by a small fin tip radius and a gradually increasing radius of curvature along the arc length. Thus, the pressure term σ/r in equation (1) has a maximum value at the fin tip, which results in a very thin condensate film near the fin tip.

With the assumption that r is sufficiently close to r_w, Gregorig[11], Fujii and Honda[12], Adamek[13] and Kedzierski and Webb[15] obtained approximate solutions for vertical finned surfaces. However, a rigorous numerical analysis shows that this assumption does not hold near the fin tip for the fin profiles proposed by Adamek[13] and Kedzierski and Webb.[15] Also, a negative value of ζ for the Adamek profile is practically impossible, because the liquid pressure at $x=0$ approaches infinity for $\zeta<0$.

Table 2 Summary of fin/interface shapes taken up for theoretical consideration.

Author	Description of fin/interface shape	Remarks
Gregorig [11]	$\frac{1}{r_w}=\frac{1.5\,\theta_t}{x_t}\left[1-\left(\frac{x}{x_t}\right)^2\right]$	Constant film thickness
Fujii and Honda [12]	Sine shape fin	Considered the effect of wall conduction
Adamek [13]	$\frac{1}{r}=\frac{\theta_t}{x_t}\left(\frac{\zeta+1}{\zeta}\right)\left[1-\left(\frac{x}{x_t}\right)^{\zeta}\right]$ where $-1\le\zeta\le\infty$	Maximum α was obtained at $\zeta=-0.5$
Mori et al.[14]	(I) Wavy fin (II) Triangular fin with round fin tip (III) Parabolic fin	Highest α was obtained by parabolic fin
Kedzierski and Webb [15]	$r=C_1+C_2\exp(Z\theta)+C_3\,\theta$ $r=r_0$ at $\theta=0$ $t_t=2\int_0^{\theta_t} r\cos\theta\,d\theta$, $h_t=\int_0^{\theta_t} r\sin\theta\,d\theta$	C_1~C_3 are obtained from geometrical conditions
Zhu and Honda [16]	(I) $r_w=a+(r_0-a)\cosh(b\theta)$ for $0\le\theta\le\theta_t(\le\pi/2)$ $X_w=t/2$ for $x_t<x$ (II) Parabolic fin (III) Rectangular fin with round corners	a and b are related by a geometrical condition Highest α was obtained by Shape I fin

Mori et al.[14] obtained numerical solutions for vertical finned surfaces with wavy, triangular and parabolic fins. Among the three classes of fin shapes considered, the highest heat transfer coeffirient was provided by the parabolic fin.

Zhu and Honda[16] obtained numerical solutions for the top and side cross-sections of horizontal finned tubes with three classes of fin shapes. Figure 2 shows a comparison of the heat transfer coefficient for CFC-11 and HCFC -123 condensing on the Shape I-III fins described in Table 2 with the same values of h and the fin spacing $s(=p-t)$. In Fig. 2, the average heat transfer coefficient for the fin cross-section at $\phi=0$ (defined on the projected area basis), α_p, is plotted against the fin tip radius r_0. It is seen from Fig. 2 that the highest heat transfer performance is provided by the Shape I fin with $r_0 \leq 0.02$ mm. Zhu and Honda[16] also showed that the optimum fin thickness for copper and brass tubes are much smaller than the actual fin thickness adopted for commercially available tubes. These results indicate that a small fin tip radius, a gradually increasing radius of curvature near the fin tip, and a small fin thickness near the fin root are essential conditions of a high-performance fin.

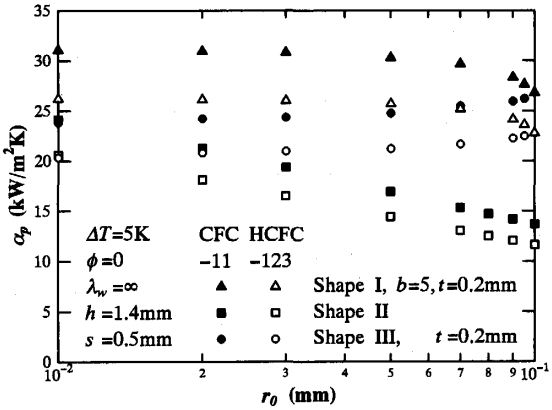

Fig. 2 Variation of α_p with r_0; comparison of Shapes I —III.

2. 2. Effect of vapor velocity

For a refrigerating machine using fluorocarbon refrigerants, the vapor velocity at the inlet of the condenser shell is designed to be 2 to 5 m/s.[17] This velocity is high enough to exert influence that can not be disregarded on the condensation heat transfer on a horizontal finned tube.

Honda et al.[18] extended the previous theoretical model for a single horizontal finned tube with conventional two-dimensional fins[7] to include the effect of vapor velocity. They assumed that the vapor shear force acting on a two-dimensional fin tube is the same as that for a smooth tube. For the thin film regions at the corner of fin tip, fin side and fin root tube surface, the regional average heat transfer coefficient, α_i, was evaluated by the equation of the form $\alpha_i=(\alpha^4_{is}+\alpha^4_{if}+\alpha^4_{ig})^{1/4}$, where α_{is}, α_{if} and α_{ig} denote the contributions due to surface tension, vapor shear and gravity, respectively. For the thick film regions at the fin tip and fin root, the circumferential condensate flow rate was calculated taking account of the vapor shear. The cross sectional area of the thick condensate film was determined by a balance of condensates flowing in and flowing circumferentially down the tube. A comparison of theoretical predictions with experimental data is shown in Fig. 8.

2. 3. Effect of condensate inundation

Recently, theoretical models that accounted for the effects of condensate inundation have been proposed by Honda et al.[19] and Murata and Hashizume[9]. Honda et al.[19] extend previous theoretical model for a single horizontal finned tube with conventional two-dimensional fins[7] to the case of a tube bundle. In this theoretical model, the effect of vapor velocity was assumed to be negligible. The condensate leaving the tube bottom was assumed to form condensate columns at low condensate flow rates, and a continuous condensate sheet at high condensate flow rates. Figure 3 shows the physical model of condensate flow in the column mode. In Fig. 3, d_r denotes the tube diameter to the fin root, d_c the tube inside diameter, d

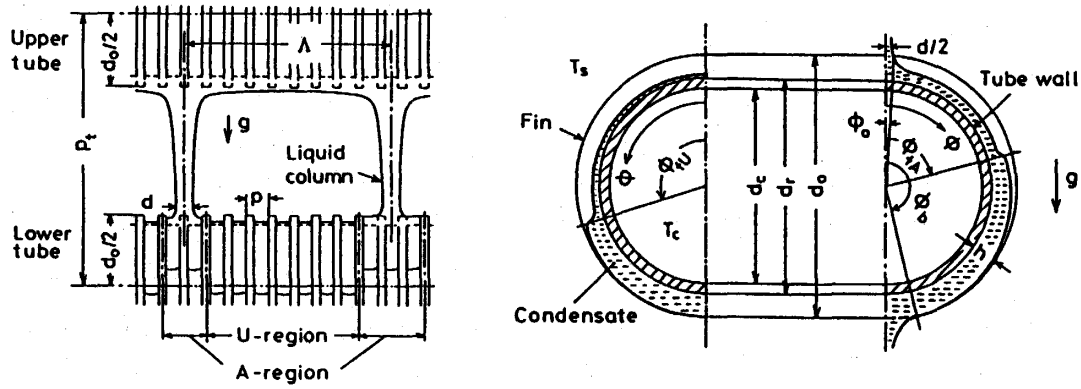

Fig. 3 Physical model of condensate flow in a tube bundle.

the diameter of impinging condensate column, p_t the vertical tube pitch, Λ the column distance, and T_c the coolant temperature. The surface of the lower tube is divided into the portion between the condensate columns and the portion under the condensate column. These portions are termed the unaffected region (U region) and the affected region (A region), respectively. Figures 3 (b) and 3 (c) show the tube cross-section in the U and A regions, respectively. The ϕ_{fU} and ϕ_{fA} denote the flooding angles below which the inter-fin space is almost completely filled with condensate. The ϕ_{fU} is determined by a balance of the surface tension and gravity forces acting on the retained condensate, whereas ϕ_{fA} is determined by a balance of the surface tension, gravity and viscous forces acting on the flowing condensate in the groove. The angular portions $0<\phi<\phi_{fU}$ and $0<\phi<\phi_{fA}$ are termed the unflooded regions (u regions), and the angular portions $\phi_{fU}<\phi<\pi$ and $\phi_{fA}<\phi<\pi$ are termed the flooded regions (f regions). Thus, in the column mode, the tube surface is divided into four regions with different characteristics, which are termed the Uu, Au, Uf and Af regions, respectively. In the sheet mode, on the other hand, the tube surface is divided into the Au and Af regions.

The average heat flux q_m, which is based on the surface area of a smooth tube with diameter d_0, is given by

$$q_m=\left[q_{Au}(\tilde{\phi}_f-\tilde{\phi}_0)_A+q_{Af}(\tilde{\phi}_b-\tilde{\phi}_f)_A\right]f+\left[q_{Uu}\tilde{\phi}_{fU}+q_{Uf}(1-\tilde{\phi}_{fU})\right](1-f) \tag{5}$$

where q_{Au}, q_{Af}, q_{Uu} and q_{Uf} are the average heat fluxes for the Au, Af, Uu and Uf regions, respectively, f is the proportion of surface area covered with the impinging condensate from the upper tube and $\tilde{\phi}=\phi/\pi$. The q_{Au}, q_{Af}, q_{Uu} and q_{Uf} values are obtained from the approximate expressions of the regional average heat transfer coefficient that are based on the numerical analysis of film condensation on a conventional two-dimensional fin tube.

Honda et al.[20] adapted the foregoing theoretical model for a bundle of conventional two-dimensional fin tubes[19] to a bundle of high-performance fin tubes proposed by Zhu and Honda[16] (i.e. Shape I fin in Table 2). A comparison of theoretical predictions with experimental data is shown in Figs. 11 and 12.

Honda and Kim[21] showed that the theoretical models proposed by Honda et al.[19,20] can be used to optimize the fin geometry. They took up the newly proposed fin tube and a rectangular fin tube for consideration and performed extensive numerical calculation with HCFC-123 as a condensing fluid. Table 3 summarizes the conditions adopted for the

Table 3 Conditions of numerical calculation.

Vapor	Substane		HCFC-123
	Saturation temperature	T_s	40 ℃
Coolant	Velocity		2.0 m/s
	Temperature	T_c	30 ℃
Tube	Geometry		Newly proposed fin, Rectangular fin, Smooth
	Material		Copper
	Diameter at fin tip	d_0	19.1 mm
	Tube Thickness	t	1.0 mm
	Vertical tube pitch	p_t	27.0 mm
	Total number of vertical tube row	n	30

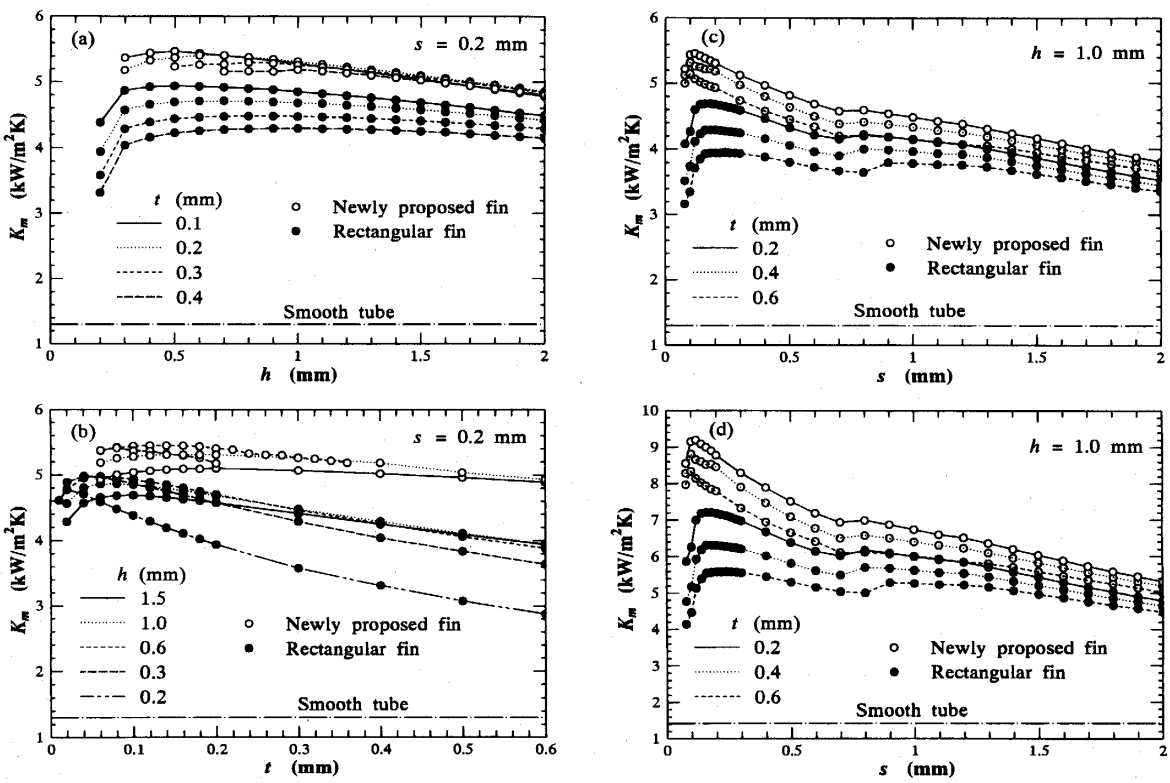

Fig. 4 Variation of K_m with h, t and s for a single tube; (a), (b), (c) without coolant side enhancement and (d) with coolant side enhancement.

numerical calculation. Figure 4 shows the effects of h, t and s on the overall heat transfer coefficient, $K_m=q_m/(T_s-T_c)$, for a single tube. Comparison of the two classes of finned tubes reveals that the K_m value is higher for the newly proposed finned tube. For this tube, the effects of h and t are rather small as compared to the effect of s. The optimum value of h ranges from 0.5 to 1.0mm, with the value increasing with t. The optimum value of t ranges from 0.08 to 0.22mm, with the value increasing with h. The optimum value of s is about 0.1mm irrespective of h and t. Figure 4 (d) shows the cases in which the coolant side heat transfer coefficient is assumed to be twice as large as that for Figs. 4 (a)-4 (c). As is

evident from the comparison of Figs. 4 (c) and 4 (d), the effect of coolant side enhancement is more significant for the newly proposed finned tube. Figure 5 shows an example of numerical results for a bundle of newly proposed fin tubes, where the overall heat transfer coefficient for a tube bundle, $\bar{K}_m=\sum_{i=1}^{n} q_{mi}/(T_s-T_c)$, is plotted as a function of s with n as a parameter. In Fig. 5, the results for a smooth tube bundle is also shown for comparison. The oblique dash-dot line in Fig.5 shows the locus of maximum $\bar{K}_m$ points for different n. As seen from the slope of this line, the optimum s value increases as n increases. Figure 6 shows the $\bar{K}_m$ value for the optimum s value, $(\bar{K}_m)_{ofs}$, plotted as a function of $s\times h$ with h and n as parameters. The $(\bar{K}_m)_{ofs}$ takes a maximum value at an intermediate value of $s\times h$ for $n\geq 3$. The dash-dot line in Fig.6 shows the locus of the maximum $(\bar{K}_m)_{ofs}$ points for different n. As expected, the optimum s and h values increase as n increases. It is also seen from the comparison of Figs. 6 (a) and 6 (b) for the newly proposed fin tube and the rectangular fin tube that the maximum value of $(\bar{K}_m)_{ofs}$ is higher for the former.

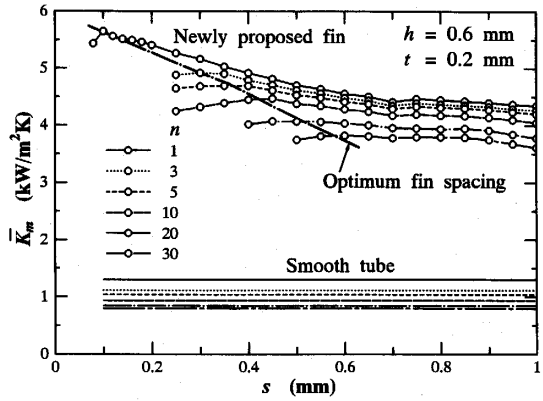

Fig. 5 Variation of $\bar{K}_m$ with s and n.

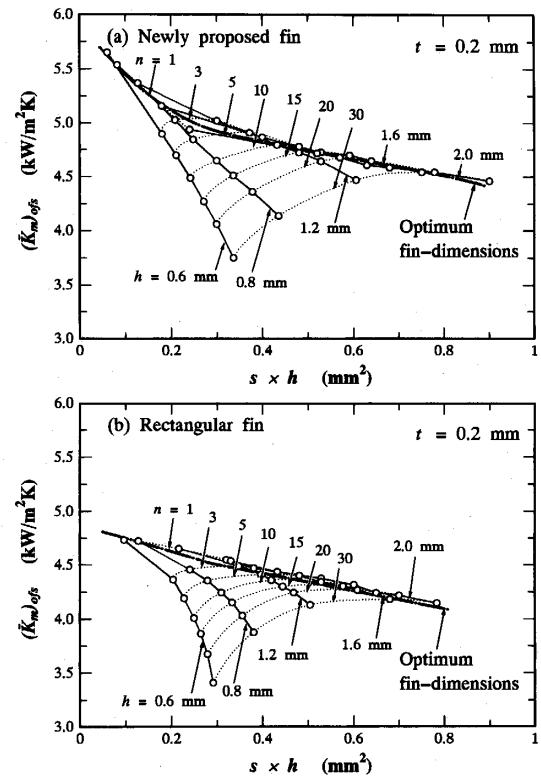

Fig. 6 Variation of $(\bar{K}_m)_{ofs}$ with $s\times h$ and n.

3. Experimental Results

3. 1. Single tube

Most of the previous experimental studies for single horizontal finned tubes have been conducted with a nearly stagnant vapor. Excellent reviews of relevant literature have been given by Webb[2], Marto[3] and Sukhatme[4].

Recently, Cavallini et al.[22] reported experimental data for downward-flowing CFC-11 and CFC-113 vapors condensing on three kinds of horizontal finned tubes. In their experiments, the test tube was assembled in a vertical duct with dummy half tubes on the side wall. Figure 7 shows the data for CFC-11, where q_m is plotted as a function of the condensation temperature difference ΔT_{in} with the vapor velocity u as a parameter. The 1333 fpm (fins per meter) tube (p=0.75mm) had a trapezoidal fin with round corners. The 2000 fpm tube (p=0.5mm) had a rectangular fin with round corners. The THERMOEXCEL tube had a saw-tooth shape fin. These tubes had surface areas 2.40, 3.26 and 2.82 times as large as that for a smooth tube with the same d_0(=15.8-18.7mm), respectively. In Fig.7, the results for a smooth tube is also presented. Comparison of the smooth and finned tubes reveals that the increase in q_m due to vapor shear is less significant for the finned tubes. The increase is smallest for THERMOEXCEL which shows the highest q_m value at low u.

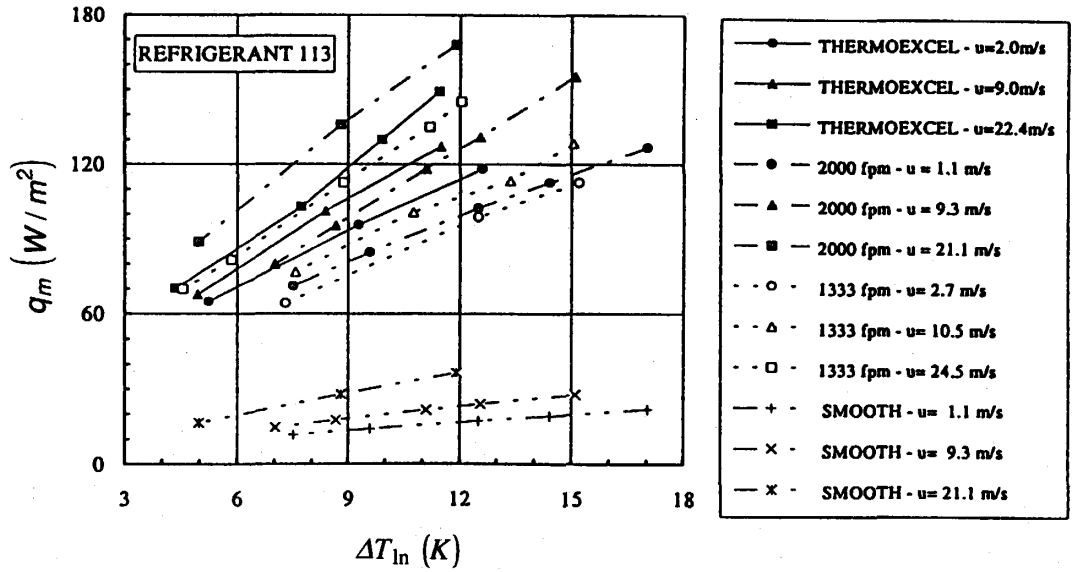

Fig. 7 Variation of q_m with ΔT_{ln}[22].

Figure 8 shows a comparison of experimental data for CFC-113 condensing on the 2000 fpm tube and predictions of Honda et al.[18] In Fig. 8, the heat transfer enhancement ratio α_m/α_N is plotted as a function of the vapor Reynolds number Re_V, where $\alpha_m=q_m/\Delta T_{ln}$ is the average heat transfer coefficient for a finned tube (based on the nominal surface area) and α_N is the average heat transfer coefficient for a smooth tube obtained from the Nusselt[5] equation. As seen from Fig. 8, the agreement is fairly good for $Re<1.5\times10^5$. However, the experimental data deviate toward a higher value for $Re_V>1.5\times10^5$. This is ascribed to the fact that the theory assumed a laminar condensate flow even for high Re_V. The triangles in Fig. 8 show the predictions of an empirical equation for the first row of a staggered bundle of horizontal smooth tubes multiplied by the finned tube to smooth tube surface area ratio[18]. While the calculated values are considerably lower than the experimental data at low Re_V, the former approaches the latter as Re_V increases. These results clearly show the change of the condensation mode on a horizontal finned tube with increasing Re_V.

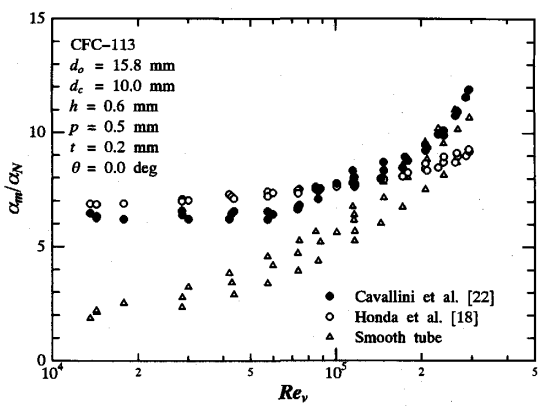

Fig. 8 Variation of α_m/α_N with Re_V; comparison of experimental data with theoretical prediction.

3. 2. Tube bundle

Recently, several experimental data have been reported for a bundle of horizontal finned tubes. Table 4 is a summary of recent studies that provide row-by-row heat transfer data. The data of Nakayama et al.,[17] Webb and Marawski[23] and Murata et al.[24] are for a nearly stagnant vapor, whereas the other data are for a vertical vapor downflow. One of the conclusions obtained from the inspection of these data is that the increase in the heat transfer coefficient due to vapor shear is much smaller for a finned tube than for a smooth tube. The increase is less significant for a tube showing a higher heat transfer coefficient at a low vapor

Table 4 Summary of recent experimental data for a tube bundle.

Author	Fluid	Tube Arrangement	Geometry
Nakayama et al.[17]	CFC-11, HCFC-22	Vertical column	1 3-d fin tube
Webb and Murawski [23]	CFC-11	Vertical column	2 2-d fin tubes 2 3-d fin tubes
Murata et al. [24]	HCFC-123	In-line bundle	1 smooth tube 2 2-d fin tubes
Honda et al.[25]	CFC-113	In-line bundle	2 2-d fin tubes 4 3-d fin tubes
Honda et al.[26]	CFC-113	Staggered bundle	2 2-d fin tubes 4 3-d fin tubes
Chu and McNaught [27]	CFC-113	Staggered bundle	1 smooth tube 2 2-d fin tubes
McNaught and Chu [28]	CFC-113	Staggered bundle	4 2-d fin tubes
Honda et al.[20]	CFC-11 HCFC-123	In-line bundle	4 2-d fin tubes
Honda et al.[29]	HCFC-123	Staggered bundle	4 2-d fin tubes

velocity. Another conclusion is that the decrease in the heat transfer coefficient due to condensate inundation is more significant for a three-dimensional fin tube than for a two-dimensional fin tube. This is attributed partly to the presence of longitudinal grooves between the three-dimensional fins, which act to equalize the condensate flow rate along the tube length. Another reason, probably more important, is that the commercially available three-dimensional fin tubes have a relatively small groove cross-sectional area, which leads to a earlier flooding of grooves with increasing condensate inundation rate.

Figure 9 shows a comparison of heat transfer performance for CFC-113 condensing in in-line and staggered bundles of six finned tubes[25]. The fin shape and dimensions of the test tubes are shown in Fig. 10 and Table 5, respectively. Tubes A and B had conventional two-dimensional fins, whereas Tubes C-F had three-dimensional fins. In Fig. 9, the condensation number for a tube row, $N_U=\alpha_m(\nu_l^2 g)^{1/3}/\lambda_l$, is plotted against the film Reynolds number $Re_f=4\Gamma/\mu_l$, where Γ is the flow rate of condensate leaving the tube bottom for one side of a tube. An overall inspection of Figs.

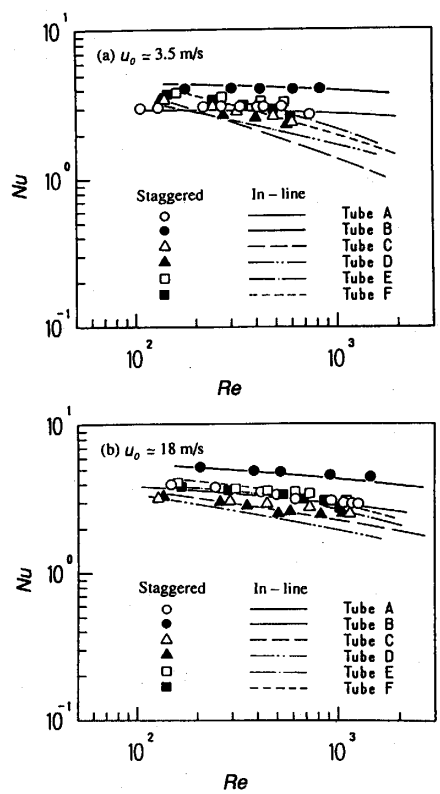

Fig. 9 Variation of Nu with Re; comparison of in-line and staggered tube bundles, CFC-113, ΔT=10K.

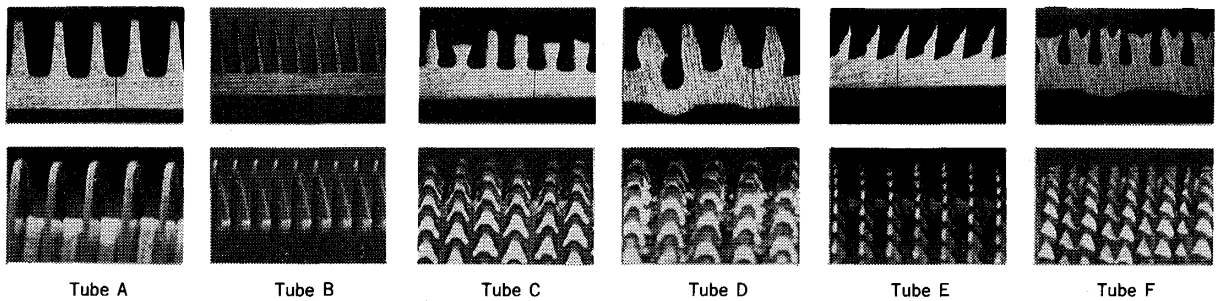

Fig. 10 Longitudinal cross section and close-up of test tubes.

Table 5 Dimensions of test tubes.

Tube designation			A	B	C	D	E	F	G	H	I
Fin pitch	p	mm	0.96	0.50	0.73	1.00	0.69	0.95	0.52	0.50	0.50
Fin height	h	mm	1.43	1.30	0.99	1.28	1.01	1.14	1.09	1.41	1.39
Fin thickness at fin root	t	mm	0.45	0.11	----	----	----	----	0.36	0.17	0.22
Radius of curvature at fin tip	r_0	mm	0.068	0.04	----	----	----	----	0.045	0.05	0.02
Fin half tip angle	θ	rad	0.082	0.047	----	----	----	----	0.062	----	----
Diameter at fin tip	d_0	mm	15.60	16.10	15.85	15.80	15.86	15.81	15.80	15.60	15.60
Tube inside diameter	d_c	mm	11.21	11.80	12.09	11.39	12.22	12.04	12.00	11.40	11.40

9 (a) and 9 (b) for different vapor velocity at the tube bundle inlet u_0 reveals that the general trend of the data is in accord with the previous conclusions regarding the effects of vapor velocity and fin geometry. The difference between the in-line and staggered bundles is insignificant for the two-dimensional fin tubes but is significant for the three-dimensional fin tubes, especially at small u_0.

Figure 11 shows a comparison of experimental data for HCFC-123 condensing in the in-line bundle of Tube A[25] and predictions of Honda et al.[19] that assumed a stagnant vapor. In Fig. 11, α_m is plotted as a function of the vertical row number n with u_0 as a parameter. At u_0=2.1 m/s, the measured α_m decreases very slowly with increasing n. These data agree with the theoretical prediction within 5%. At u_0=4.2 and 7.5 m/s, the measured α_m decreases sharply from the first row to the fourth row, and then it decreases very slowly with further increasing n. It is seen from Fig. 11 that the effect of vapor velocity is insignificant for $n \geq 6$.

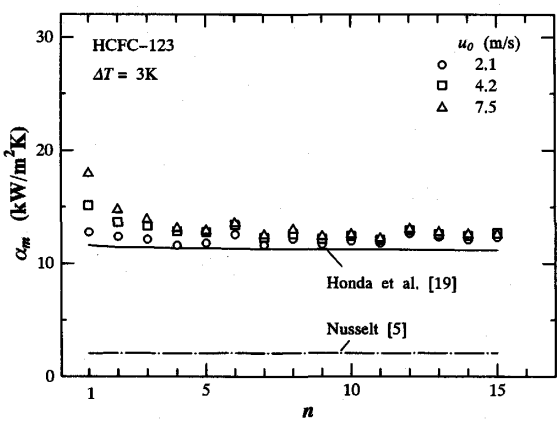

Fig. 11 Variation of α_m with n; comparison of experimental data with theoretical prediction.

Figure 12 shows a comparison of in-line and staggered tube bundles[29], where the α_m value for HCFC-123 condensing in the bundles of four kinds of two-dimensional fin tubes is plotted as a function of Γ. The fin shape and dimensions of the test tubes are shown in Fig. 13 and Table 5, respectively. Tubes A and G had conventional two-dimensional fins, whereas

Tubes H and I had fin shapes close to the high-performance fin proposed by Zhu and Honda[16]. Since Tube A in Fig. 12 is the same as that in Fig. 10, the data for Tube A can be used as a basis of the evaluation of heat transfer performance among TubesA - I. Inspection of Figs. 10 and 12 reveals that the highest heat transfer performance, about 73% higher than the staggered bundle of Tube A, is provided by the staggered bundle of Tube H. This indicates the usefulness of the procedure for the optimization of fin geometry described in section 2. 3. The solid and dotted lines in Fig. 12 show theoretical predictions of Honda et al.[19,20] Generally, the theoretical prediction agrees fairly well with the measured data. However, there exist two problems with the theoretical models. First, while the measured α_m decreases monotonically with increasing Γ, the predicted α_m shows a discontinuity at $\Gamma \cong 0.05$ kg/m s. This is caused by the change in the condensate inundation mode (i.e. column mode to sheet mode) assumed in the theoretical model. Second, the theoretical prediction deviates toward a smaller value as Γ increases. The theory needs to be modified to take account of the effects of vapor shear and momentum of falling condensate.

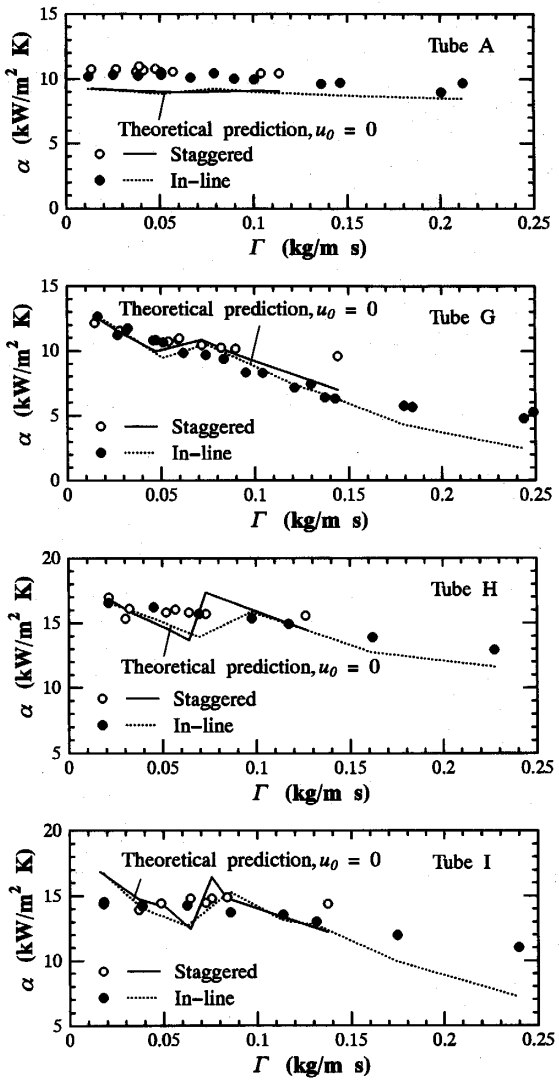

Fig. 12 Variation of α_m with Γ; comparison of in-line and staggered tube bundles, HCFC-123, u_0=4m/s, ΔT =8K.

Conclusions

Recently, significant advances have been made in understanding the effects of fin geometry, vapor shear and condensate inundation on the film condensation of fluorocarbon refrigerants in a bundle of horizontal finned tubes. Several advanced two-dimensional fin shapes that can utilize the surface tension effects efficiently have been proposed. Theoretical studies show that a small fin tip radius, a gradually increasing radius of curvature along the arc length, and a small thickness at the fin root are essential conditions of a high-performance fin. The optimum fin height and the optimum fin spacing increase with the vertical bundle depth.

The effect of vapor shear is much smal-

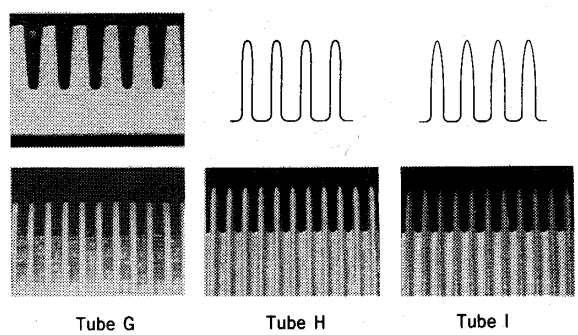

Fig. 13 Close-up and longitudinal cross section of test tubes

ler for a finned tube than for a smooth tube. The effect is even smaller for the lower row of two-dimensional fin tubes. The effect of condensate inundation is more marked for a three-dimensional fin tube than for a two-dimensional fine tube. Also, the effect is more marked for an in-line tube bundle than for a staggered tube bundle.

For a single two-dimensional fin tube with and without the effect of vapor shear, several theoretical models exist that can predict the heat transfer coefficient with sufficient accuracy. For a tube bundle, the theoretical prediction is satisfactory for small to medium condensate inundation rates and negligible vapor shear.

Experimental studies reporting on the heat transfer performance of pure alternative refrigerants are still limited. No data is available for mixtures of alternative refrigerants. More data are needed for these fluids.

The author is grateful to Mr. N. Takada and Mr. O. Makishi for their help in preparing this paper.

References

1) R. L. Webb, ASHRAE Trans., 90, Pt. 1 (1984), 5.
2) R. L. Webb, Int. Comm. Heat Mass Transf. 15, 4 (1988), 475.
3) P. J. Marto, Trans. ASME, J. Heat Transf., 110, 4 (B) (1988), 1287.
4) S. P. Sukhatme, Proc. 9th Int. Heat Transf. Conf., 1 (1990), 305.
5) W. Nusselt, Zeit. Ver. Deut. Ing., 66 (1916), 541, 569.
6) K. O. Beatty, Jr. and D. L. Katz, Chem. Engg. Prog., 44, 1 (1948), 55.
7) H. Honda, S. Nozu and B. Uchima, JSME Int. J., Ser. 2, 31, 4 (1988), 709.
8) T. Adamek and R. L. Webb, Int. J. Heat Mass Transf., 33, 8 (1990), 1721.
9) K. Murata and K. Hashizume, Experimental Heat Transf., 5, 1 (1992), 115.
10) J. W. Rose, Condensation and Condenser Design, ASME, New York, (1993), 317.
11) R. Gregorig, Z. Angew. Math. Phys., 5 (1954), 36.
12) T. Fujii and H. Honda, Proc. 6th Int. Heat Transf. Conf., 2 (1978), 419.
13) T. Adamek, Wärme-Stoffübertrag., 15 (1981), 255.
14) Y. Mori, K. Hijikata, S. Hirasawa and W. Nakayama, Trans. ASME, J. Heat Transf., 103, 1 (1981), 96.
15) M. A. Kedzierski and R. L. Webb, Trans. ASME, J. Heat Transf., 112, 2 (1990), 479.
16) H. Zhu and H. Honda, Trans. JSME, Ser. B, 58, 11 (1992), 3464.
17) W. Nakayama, K. Takahashi, T. Senshu and H. Yoshida, ASHRAE Trans., 90, Pt. 1 (1984), 60.
18) H. Honda, K. H. Kim and T. Madanbashi, Proc. 30th Heat Transfer. Symp. Japan, 1 (1993), 352.
19) H. Honda, S. Nozu and Y. Takeda, Trans. ASME, J. Heat Transf., 111, 2 (1989), 525.
20) H. Honda, H. Takamatsu and K. H. Kim, J. Enhanced Heat Trasf., 1, 2 (1994), 197.
21) H. Honda and K. H. Kim, Proc. 1993 ICHMT Int. Symp. on New Developments in Heat Exchangers, 3. 1 (1993); also J. Enhanced Heat Transf., 1, 3 (1994) (in press).
22) A. Cavallini, G. A. Longo and L. Rosetto, Proc. Int. Seminar on Heat Transfer, Thermophysical Properties and Cycle Performance of Alternative Refrigerants, (1993), 57.
23) R. L. Webb and C. G. Murawski, Trans. ASME, J. Heat Transf., 112, 3 (1990), 768.
24) K. Murata, N. Abe and K. Hashizume, Proc. 9th Int. Heat Transf. Conf., 4 (1990), 259.
25) H. Honda, B. Uchima, S. Nozu, H. Nakata and E. Torigoe, Trans. ASME, J. Heat Transf., 113, 2 (1991), 479.
26) H. Honda, B. Uchima, S. Nozu, E. Torigoe and S. Imai, Trans. ASME, J. Heat Transf.,

114, 2 (1992), 442.
27) C. M. Chu and J. M. McNaught, Inst. Chem. Engrs. Symp. Ser., 129 (1992), 225.
28) J. M. McNaught and C. M. Chu, Condensation and Condenser Design, ASME, New York, (1993), 367.
29) H. Honda, H. Takamatsu, O. Makishi, H. Sejimo and N. Takada, Proc. 31th Heat Transf. Symp. Japan, 2 (1994), 739.